

Article

Characterization of Cu(II) and Zn(II) Sorption onto Zeolite

Tomáš Bakalár ^{1,*} , Henrieta Pavolová ¹, Kamil Kyšela ² and Zuzana Hajduová ³ 

¹ Institute of Earth Resources, Faculty of Mining, Ecology, Process Control and Geotechnologies, Technical University of Košice, Letná 9, 042 00 Košice, Slovakia; henrieta.pavolova@tuke.sk

² Institute of Geodesy, Cartography and Geographical Information Systems, Faculty of Mining, Ecology, Process Control and Geotechnologies, Technical University of Košice, Letná 9, 042 00 Košice, Slovakia; kamil.kysel@tuke.sk

³ Faculty of Business Management, University of Economics in Bratislava, Dolnozemska cesta 1/b, 852 35 Bratislava, Slovakia; zuzana.hajduova@euba.sk

* Correspondence: tomas.bakalar@tuke.sk

Abstract: In this study, a batch sorption study approach was combined with an instrumental analytical approach of atomic absorption spectroscopy, X-ray diffraction (XRD) and X-ray photoelectron spectroscopy (XPS) for the sorption of copper and zinc ions from aqueous solution on zeolites. Both copper and zinc are biogenic elements; nevertheless, many industrial processes produce an excessive amount, which is why their efficient removal from water must be studied. Two types of zeolites, Zeolite Micro 20 (Z-M20) and Zeolite Micro 50 (Z-M50), were used. The results showed that the maximum sorption capacities for removal of Cu and Zn were 1.06 for CuSO₄, 42.35 for Cu(NO₃)₂, 1.15 for ZnSO₄ and 2.29 for Zn(NO₃)₂ adsorption onto Z-M20 and 0.45 for CuSO₄, 1.67 for Cu(NO₃)₂, 0.39 for ZnSO₄ and 1.51 for Zn(NO₃)₂ adsorption onto Z-M50. The maximum sorption capacities are higher for sulfates and the sorbent with smaller particle size. The sorption capacities of Cu and Zn for corresponding anion and particle size differ only up to 5–15%. Using XRD and XPS analyses before and after the sorption process, it was found that the content of both Cu and Zn in the surface layer and the bulk are the same for sorption onto sorbent with smaller particle size, but are higher in the surface layer than in the bulk for sorption onto sorbent with larger particle size. One of the main findings of this study is that a zeolite with smaller particles takes Cu and Zn by the whole particle, while with bigger particles, Cu and Zn concentrate in the surface of the particle. The results of the study may be used as an indicator for sorption efficiency of the studied zeolites for their application in the treatment of copper and zinc contaminated effluents.

Keywords: zeolite; sorption; Cu(II); Zn(II); surface layer; bulk



Citation: Bakalár, T.; Pavolová, H.; Kyšela, K.; Hajduová, Z. Characterization of Cu(II) and Zn(II) Sorption onto Zeolite. *Crystals* **2022**, *12*, 908. <https://doi.org/10.3390/cryst12070908>

Academic Editor:
Younes Hanifepour

Received: 6 June 2022
Accepted: 23 June 2022
Published: 25 June 2022

Publisher's Note: MDPI stays neutral with regard to jurisdictional claims in published maps and institutional affiliations.



Copyright: © 2022 by the authors. Licensee MDPI, Basel, Switzerland. This article is an open access article distributed under the terms and conditions of the Creative Commons Attribution (CC BY) license (<https://creativecommons.org/licenses/by/4.0/>).

1. Introduction

Zeolite–clinoptilolite is a natural rock with exceptional physical properties resulting from its special crystal structure. The extensive use of zeolite results mainly from the specific physico-chemical properties, such as high ion exchange capacity and selectivity, reversible hydration and dehydration, high gas sorption capacity, high thermostability, resistance to aggressive environments, highly specific surface, etc. [1]. For these properties it has been widely used for heavy metal sorption and removal from water. Copper and zinc are biogenic elements, two of the essential trace elements for humans and plants and participate in enzymatic reactions in organisms. However, their surplus is harmful to living organisms, their compounds may pose toxic to aquatic organisms [2,3].

Copper ions (Cu) and zinc ions (Zn) removal from aqueous solutions is widely studied. Different methods have been developed for the removal of Cu and Zn [4] including methods such as precipitation [5,6], membrane separation [7–9], coagulation and flocculation [10,11], biosorption [12–14], ion-exchange [13,15], adsorption [16–18], combined processes [19], etc. Sorption is considered as one of the promising methods to remove

Cu and Zn from wastewater for easy application and recyclability of the sorbents [20,21]. The sorption capacity of zeolite is significantly influenced by pH, temperature, particle size distribution, etc., and studies mostly concentrate on the solution. The Cu sorption capacity of magnetic nano-zeolite is increasing with increasing pH [22]. NaP zeolite from waste lithium-silica-powder and NaX zeolite from aluminate and silicate solutions both prepared by hydrothermal method proved as efficient Cu sorbent and their sorption capacities also increased with increasing pH and temperature [23,24]. Equilibrium studies of heavy metal sorption by zeolite synthesized from a combination of oil shale ash and coal fly ash determined the selectivity in order: Pb > Cr > Cu > Cd > Zn [25]. The maximum sorption capacity of zeolite from the Yagodninsk deposit of the Kamchatka region was in order Cu > Fe > Ni > Co [26], of FAU-type zeolite from coal fly ash was in order Pb > Cu > Cd > Zn > Co [27]. For a comparison, the order of Ni > Mn > Zn > Cu > Cd = Pb for montmorillonite and the order of Mn > Ni > Zn > Cd > Cu > Pb for vermiculite were recorded [28]. The maximum sorption capacity for Zn sorption was in order Zeolite 3A > Zeolite 10A > Zeolite 13X > Natural Zeolite [29]. Based on recent research, zeolite is, except heavy metals, also used for U sorption [30], I[−] sorption [31] and petroleum substances sorption [32]. A relatively new approach to zeolites with adsorbed Cu proved antibacterial activity [33].

As mentioned above, most of the studies concentrate only on the study of sorption processes based on the aqueous phase. For this reason, this study also focuses on the solid phase, especially in the surface layer. The sorption of Cu and Zn ions onto natural zeolites from local source in Slovakia was studied in batch experiments. The solutions were analyzed for Cu and Zn concentrations and Langmuir, Freundlich and Redlich–Peterson adsorption isotherms apply. Cu and Zn saturated solid samples were analyzed for elemental composition by X-ray diffraction (XRD) and X-ray photoelectron spectroscopy (XPS) to consider the sorption process and the exchange of cations. In this study, the aim was to use the natural unmodified form to study the sorption process not only based on the results from the aqueous solution, but also the solid residue after the sorption that is often neglected.

2. Materials and Methods

Zeolites were provided by Zeocem, a.s. (Bystré, Slovakia). Zeolite Micro 20 (Z-M20) and Zeolite Micro 50 (Z-M50) were used in the study and were not modified. The initial Cu and Zn solutions were prepared with analytical grade CuSO₄·5H₂O, Cu(NO₃)₂·3H₂O and ZnSO₄·7H₂O, Zn(NO₃)₂·6H₂O, respectively, provided by CENTRALCHEM, s.r.o. (Bratislava, Slovakia).

Zeolites. The samples were analyzed for particle size distribution by a particle sizer Analysette 22 (Fritsch, Germany). The Sauter mean diameter of particles, defined as

$$d_{32} = \frac{\sum(n_i d_i^3)}{\sum(n_i d_i^2)}, \quad (1)$$

n_i is the mass percentage of i -th fraction (%), d_i is the mean particle size of i -th fraction (m), can be considered mean particle size.

In the equilibrium experiments a series of flasks with a volume of 0.1 dm³ (V) of metal ion solution of different initial concentrations ($C_0 = 1$ to 2000 mg·dm^{−3}) prepared from copper and zinc salts and a fixed dosage of sorbent ($C_a = 1$ g·dm^{−3}) were agitated in a rotary shaker at 200 rpm and 25 °C for 2 h to reach an equilibrium [34,35]. The initial solution pH was not adjusted. The equilibrated, sedimented samples and filtered samples were analyzed for metal content by Atomic absorption spectroscopy (AAS). The solid samples were analyzed by XRF and XPS. The adsorbed metal concentrations q_e (mg·g^{−1}) were calculated as the difference of the initial metal concentration C_0 (mg·dm^{−3}) and equilibrium metal concentration C_e (mg·dm^{−3}) in the solution:

$$q_e = (C_0 - C_e) \times V / m_a, \quad (2)$$

m_a (g) is the weight of sorbent, and V (L) is the volume of solution.

For optimization of the use of sorbents isotherm models provide an adequate description of metal ions sorption equilibria on zeolites.

Freundlich isotherm [36]:

$$q_e = K_f \times C_e^{1/n}, \quad (3)$$

K_f ($\text{mg}^{1-n} \cdot \text{L}^n \cdot \text{g}^{-1}$) is adsorption equilibrium constant, n (1) is a constant related to the intensity of the adsorption; the isotherm represents sorption taking place on a heterogeneous surface with interaction between the adsorbed molecules [37].

Langmuir isotherm [38]:

$$q_e = q_m \times a_L \times C_e / (1 + a_L \times C_e), \quad (4)$$

q_m ($\text{mg} \cdot \text{g}^{-1}$) is maximum sorption capacity, a_L ($\text{dm}^3 \cdot \text{mg}^{-1}$) is adsorption energy; the isotherm represents sorption taking place on a homogenous surface within the sorbent [39].

Redlich–Peterson isotherm [40]:

$$q_e = K_R \times C_e / (1 + a_R \times C_e^\beta), \quad (5)$$

K_R ($\text{dm}^3 \cdot \text{g}^{-1}$) and a_R ($\text{dm}^{3\beta} \cdot \text{g}^{-\beta}$) are constants, β (1) is exponent; the isotherm is used as compromise between the Langmuir and Freundlich systems [37].

Flame AAS, using iCE 3300 (ThermoFisher Scientific, Grand Island, NY, USA) performed the metal concentration analyses in solutions. XPS, using PHOIBOS 100 SCD (SPECS Surface Nano Analysis GmbH, Berlin, Germany) model equipped with a non-monochromatic X-ray source measured at 70 eV transition energy and high-resolution spectra at 50 eV, performed the analyses of solid samples at room temperature. XRF, using SPECTRO iQ II (SPECTRO Analytical Instruments GmbH, Kleve, Germany) with SDD silicon drift detector with resolution of 145 eV at 10,000 pulses, performed the chemical composition of tested samples. The latter two non-invasive techniques are analyzing the composition of material with a difference in the depth of scanning—XPS has a depth resolution in first 10 nm, XRF enables a bulk analysis and has depth sensitivity [41,42].

Each of the experiments was performed three times and the result was taken as the average value.

3. Results

Two types of zeolite were used, Z-M20 with an average particle size of 20 μm and a particle size distribution in the range of 0–90 μm and Z-M50 with an average particle size of 50 μm and a particle size distribution in the range of 0–350 μm . The clinoptilolite content was 60–65%. Other compounds were cristobalite, clay mica, plagioclase and rutile [1]. The Sauter mean diameter anticipating spherical shape of particles is different from the arithmetical mean diameter of sorbent particles (d_{50}), a simple mean irrespective of shape. The surface area of particles is similar. The basic physical properties of the used materials are presented in Table 1.

Table 1. The basic physical properties of zeolites.

Parameter	Z-M20	Z-M50
Particle size (μm)	0–90	0–350
d_{32} (μm)	19.553	50.862
d_{50} (μm)	3.493	9.549
Surface area ($\text{m}^2 \cdot \text{g}^{-1}$)	25.84	26.33

Abbr.: Z-M20—Zeolite Micro 20; Z-M50—Zeolite Micro 50.

The basic chemical compositions of zeolites and zeolites after sorption are presented in Table 2. The Cu and Zn solution concentrations used for the comparison were selected so that the removal efficiencies were in the range of 5–7%.

Table 2. The basic chemical composition of zeolites.

Compound (wt.%)	Z-M20 *	Z-M20				Z-M50 *	Z-M50			
		CuSO ₄	Cu(NO ₃) ₂	ZnSO ₄	Zn(NO ₃) ₂		CuSO ₄	Cu(NO ₃) ₂	ZnSO ₄	Zn(NO ₃) ₂
SiO ₂	51.54	51.58	51.21	51.58	52.08	54.33	54.66	53.70	53.07	53.90
Al ₂ O ₃	8.66	9.30	8.92	9.15	8.25	7.35	7.36	7.17	7.62	7.27
CaO	1.79	1.38	1.39	1.79	1.85	1.26	0.83	0.98	1.38	1.35
K ₂ O	1.36	1.13	1.12	1.32	1.20	1.45	1.39	1.51	1.34	1.47
Fe ₂ O ₃	0.91	0.17	0.59	0.03	0.03	0.08	0.02	0.07	0.00	0.02
FeO	0.10	0.11	0.09	0.01	0.02	0.10	0.03	0.10	0.01	0.02
SeO ₂	0.14	0.14	0.14	0.13	0.13	0.55	0.51	0.51	0.49	0.49
CuO	0.00	0.22	0.45	0.00	0.00	0.00	0.09	0.33	0.00	0.00
ZnO	0.00	0.00	0.00	0.23	0.43	0.00	0.00	0.00	0.08	0.31

* Z-M20 and Z-M50—before sorption; the rest are respective zeolites after sorption.

The particle size distributions of both Z-M20 and Z-M50 are normal (Gaussian) distributions though the particle size is different. The particle size and its distribution may affect the sorption process and the amount of adsorbed Cu and Zn [43].

The equilibrium data and the fitted data of Cu and Zn sorption by Freundlich, Langmuir, and Redlich–Peterson isotherms are presented in Figures 1 and 2, respectively. The maximum sorption capacities are presented in Table 3.

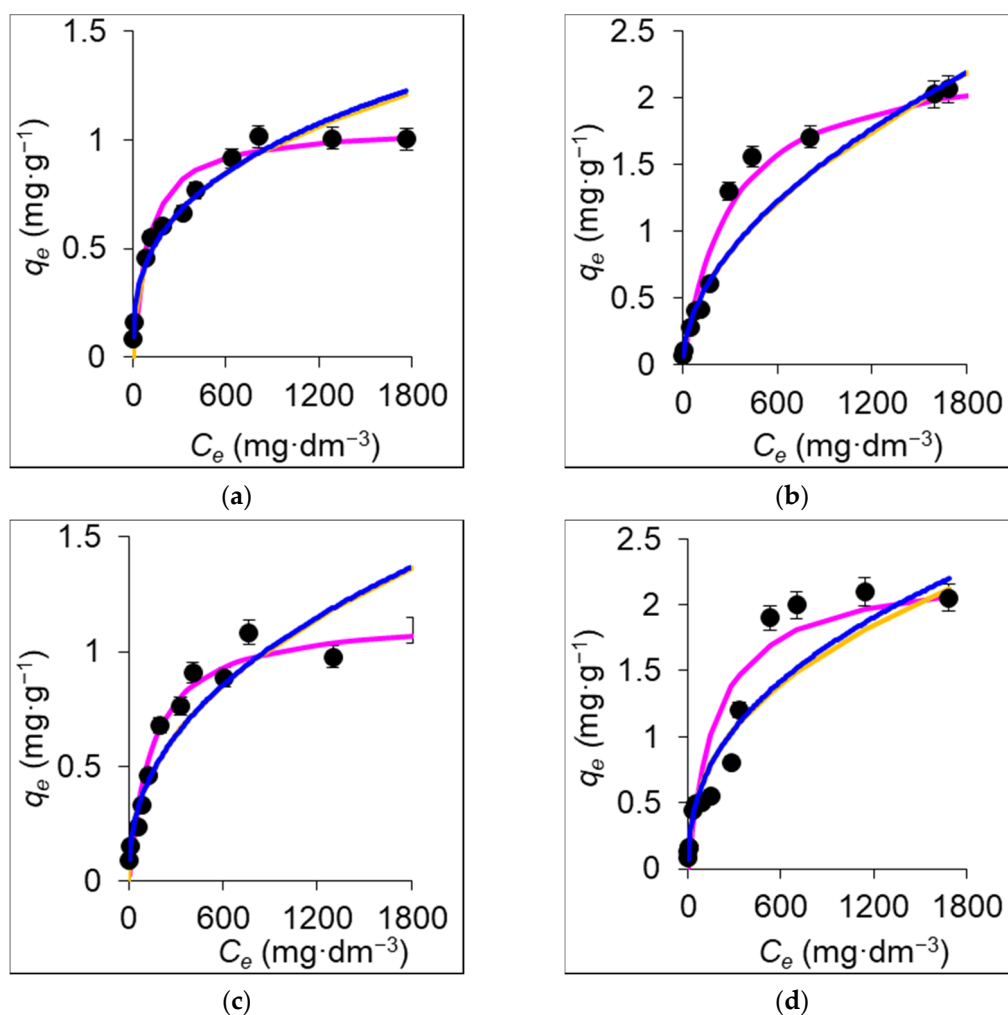


Figure 1. Experimental data of Cu sorption on Z-M20 from (a) CuSO₄ (b) Cu(NO₃)₂, and Zn sorption on Z-M20 from (c) ZnSO₄ (d) Zn(NO₃)₂. Note: black dots—experimental data ± standard deviation; blue line—Freundlich isotherm, pink line—Langmuir isotherm, orange line—Redlich–Peterson isotherm.

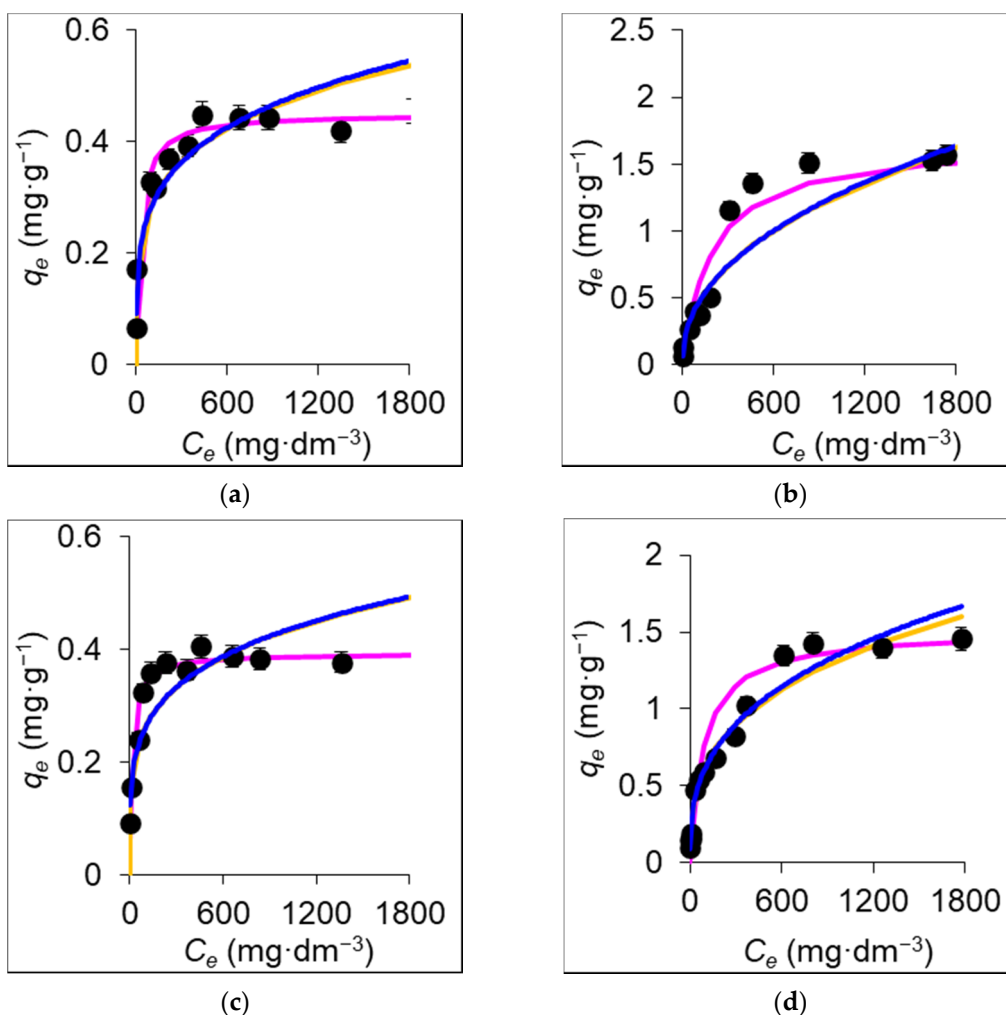


Figure 2. Experimental data of Cu sorption on Z-M50 from (a) CuSO_4 (b) $\text{Cu}(\text{NO}_3)_2$, and Zn sorption on Z-M50 from (c) ZnSO_4 (d) $\text{Zn}(\text{NO}_3)_2$. Note: black dots—experimental data \pm standard deviation; blue line—Freundlich isotherm, pink line—Langmuir isotherm, orange line—Redlich–Peterson isotherm.

Table 3. Adsorption isotherm parameters of Cu and Zn on zeolites.

Isotherm	Parameter	Z-M20				Z-M50			
		CuSO_4	$\text{Cu}(\text{NO}_3)_2$	ZnSO_4	$\text{Zn}(\text{NO}_3)_2$	CuSO_4	$\text{Cu}(\text{NO}_3)_2$	ZnSO_4	$\text{Zn}(\text{NO}_3)_2$
Freundlich	$K_f \cdot \text{mg}^{1-n} \cdot \text{dm}^{3n} \cdot \text{g}^{-1}$	0.10	0.04	0.05	0.10	0.10	0.06	0.11	0.13
	n	2.94	1.89	2.33	2.38	4.43	2.24	5.70	2.89
	R^2	0.95	0.89	0.88	0.94	0.88	0.84	0.75	0.96
Langmuir	$q_m \cdot \text{mg} \cdot \text{g}^{-1}$	1.06	2.35	1.15	2.29	0.45	1.67	0.39	1.51
	$a_L \cdot \text{dm}^3 \cdot \text{mg}^{-1}$	0.011	0.003	0.007	0.005	0.035	0.005	0.061	0.011
	R^2	0.98	0.99	0.98	0.94	0.97	0.97	0.97	0.94
Redlich–Peterson	$K_R \cdot \text{dm}^3 \cdot \text{g}^{-1}$	0.83	0.78	0.80	0.77	1.01	0.93	1.55	0.99
	$b_R \cdot \text{dm}^{3\beta} \cdot \text{g}^{-\beta}$	7.92	18.30	14.17	6.99	9.33	15.46	16.00	6.88
	β	0.67	0.47	0.58	0.60	0.79	0.56	0.78	0.68
	R^2	0.98	0.94	0.94	0.96	0.95	0.92	0.87	0.98

The coefficients of determination (R^2) are in the range of 0.75 to 0.99 (Table 3). Based on the regression analysis and fit in the graphics, the experimental data are fit by Lagmuir isotherm the most accurately for sorption of Cu from both CuSO_4 and $\text{Cu}(\text{NO}_3)_2$ onto both Z-M20 and Z-M50. It presumes that the Cu ions are adsorbed on a fixed number of sites

on the zeolites, each site is occupied by one adsorbed ion, all the sites are energetically equivalent, the sorption is monolayer, and the adsorbed molecules do not interact [43,44]. The most accurate fit is also by Langmuir isotherm for sorption of Zn from ZnSO₄ onto both Z-M20 and Z-M50, which means that the sorption process assumes the same features as the Cu sorption onto the zeolites. The only exception to the above-mentioned is the best accuracy of fit by Redlich–Peterson isotherm for sorption of Zn ions from Zn(NO₃)₂ onto both Z-M20 and Z-M50. The sorption process described by Redlich–Peterson isotherm combines elements from both Langmuir and Freundlich equations. The mechanism of sorption is a mix, does not follow ideal monolayer sorption. It is applicable in both homogenous or heterogeneous systems due to its versatility [45]. When considering the maximum sorption capacities:

- The difference between Cu and Zn sorption is less than 15% for both sulfates and nitrates and Z-M20 and Z-M50;
- There is a statistically significant difference between the sorption of Cu from CuSO₄ and Cu(NO₃)₂ and of Zn from ZnSO₄ and Zn(NO₃)₂ for both Z-M20 and Z-M50;
- The maximum sorption capacity is higher for sorption from nitrates than from sulfates;
- The maximum sorption capacity is higher for Z-M20 and Z-M50.

In general, the maximum sorption capacities are higher for sulfates and Z-M20 than nitrates and Z-M50.

The XPS scan spectra are shown in Figure 3. The original Z-M20 and Z-M50 XPS spectra outlines the typical dominance of O 1s—oxygen that can be found throughout the zeolite together with Si 2p—silicon and Al 2p—aluminum. There is also a higher content of Ca 2p—calcium and Se 3d—selenium, followed by K 2p—potassium, Ca 2p—calcium, and Fe 2p—iron. There is only a slight difference between Z-M20 and Z-M50 in the occurrence of the elements. As mentioned above the XPS analyses detect relevant elements on the surface layer that are confirmed by the XRF analyses with the aluminosilicate structure Si/Al (weight rate) = 4.94 and 5.77 [Si/Al (molar rate) = 5.14 and 6.00] on average for Z-M20 and Z-M50, respectively. This ratio is constant irrespectively of Cu or Zn amount adsorbed. The content of Si is 24.77% and 24.69%, and of Al is 4.82% and 4.14%, for Z-M20 and Z-M50, respectively, on average. The content of the rest of the elements (Fe, Ca, Se and K) in pure samples is different for both Z-M20 and Z-M50. For pure Z-M20, Ca has the highest content followed by K, the content of Fe and Se is significantly lower, confirmed by both XPS and XRF measurements. It means that the composition is similar in both the surface layer and the bulk. For pure Z-M50, K has the highest content followed by much lower content of Ca, Fe and Se, also confirmed by both XPS and XRF measurements, indicating the similarity of the composition in both the surface layer and the bulk, too. There is no Cu or Zn in the pure zeolite samples. The content of Cu and Zn in the surface layer and in the bulk is different after the sorption though some similarities were discovered and is also discussed in Discussion section:

- The contents of Cu adsorbed from both CuSO₄ and Cu(NO₃)₂ onto Z-M20 in the surface layer and the bulk are the same;
- The content of Cu adsorbed from both CuSO₄ and Cu(NO₃)₂ onto Z-M50 in the surface layer is several times higher than in the bulk;
- The contents of Zn adsorbed from both ZnSO₄ and Zn(NO₃)₂ onto Z-M20 in the surface layer and the bulk are the same;
- The content of Zn adsorbed from both ZnSO₄ and Zn(NO₃)₂ onto Z-M50 in the surface layer is higher than in the bulk.

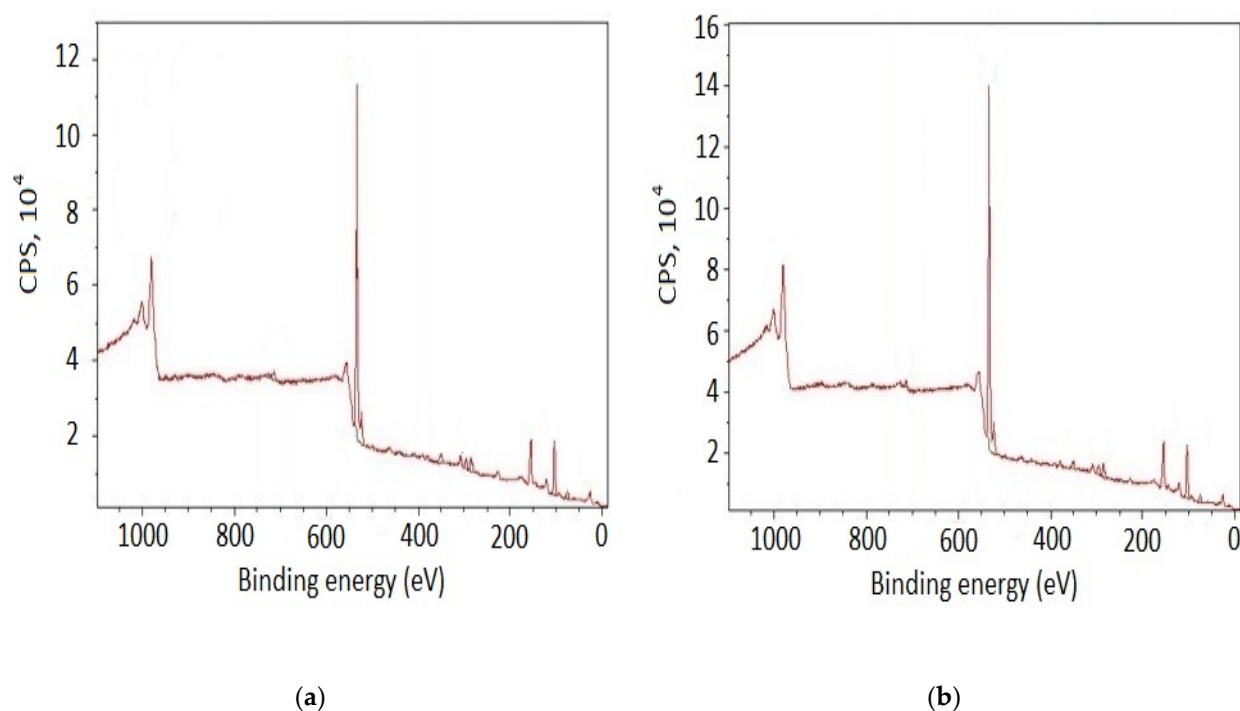


Figure 3. XPS analyses of (a) Z-M20, and (b) Z-M50.

4. Discussion

The content of not only Cu and Zn on the surface and in the bulk of the zeolite might be different as discussed in the Materials and Methods section. The content of Cu and Zn is presented in Tables 4 and 5, respectively.

Table 4. A comparison of Cu content in $\text{mg}\cdot\text{g}^{-1} \pm$ standard deviation.

Method	Source	Z-M20		Z-M50	
		CuSO ₄	Cu(NO ₃) ₂	CuSO ₄	Cu(NO ₃) ₂
XPS		1.02 ± 0.05	2.11 ± 0.11	1.67 ± 0.08	13.40 ± 0.67
XRF		1.01 ± 0.05	2.09 ± 0.10	0.44 ± 0.02	1.54 ± 0.08
Adsorbed		1.01 ± 0.05	2.13 ± 0.11	0.44 ± 0.02	1.54 ± 0.08

Table 5. A comparison of Zn content in $\text{mg}\cdot\text{g}^{-1} \pm$ standard deviation.

Method	Source	Z-M20		Z-M50	
		ZnSO ₄	Zn(NO ₃) ₂	ZnSO ₄	Zn(NO ₃) ₂
XPS		1.00 ± 0.05	2.05 ± 0.10	0.99 ± 0.05	2.00 ± 0.05
XRF		1.10 ± 0.06	2.05 ± 0.10	0.38 ± 0.02	1.46 ± 0.07
Adsorbed		1.09 ± 0.05	2.05 ± 0.10	0.39 ± 0.02	1.46 ± 0.07

The sorption process of both Cu and Zn onto zeolites is similar when evaluated based on the contents of Zn and Cu in the solid phase after sorption though the concentrations are different. There is no difference in concentration of the adsorbed metals between data from XPS and XRF for the sorption of both Cu and Zn onto Z-M20. This might imply that the metals are adsorbed evenly on the surface and in the bulk. Though the concentration of adsorbed metals is different from XPS and XRF for the sorption of both Cu and Zn onto Z-M50. The concentration on the surface (the data from XPS) is significantly higher than the concentration in the bulk (the data from XRF), which might imply that more metal is adsorbed in the surface than below the surface layer, but the total concentration is almost equal to the adsorbed amount. The difference in the sorption behavior between Z-M20 and Z-M50 might be caused by the particle size as the adsorbed metals are equally

distributed throughout the smaller particles while the adsorbed metals can be found in higher concentration on the surface than below the surface in the large ones.

In case of NaP zeolite prepared from waste lithium-silica-powder by hydrothermal method and synthesized NaX nanoparticles, Cu in the solution was ion-exchanged for Na ion on the surface and interaction was between the hydrate water in the solid phase and Cu [23,24]. The situation was similar for Analyses of Cu sorption onto zeolites synthesized from Greek fly ash proved that copper occurred in the zeolitic framework including open channels and Cu(II) oxidation state occurred in the due to the formation of CuO and/or Cu-Cl [46]. In case of Chilean zeolite after acid treatment and Cu sorption, 46.69% of the zeolite sample was copper as sodium exchanged with Cu [33]. Cu sorption onto zeolites is not only predominantly cation exchange, but also close to stoichiometric cation exchange values of equilibrium sorption amounts. It was also proved that zeolites with larger pores enabled increased sorption amount and enhanced sorption capacity also for cations with larger diameters [34].

The influence of cation size on the sorption process was also proved as Zn replace the cations inside the bulk more than Pb with a much larger size. The desorption of Pb is higher because Zn are exchanged more with the ions in the bulk than in the surface layer during the sorption. Due to their size Pb do not penetrate the pores and channels as much as Zn, thus their desorption is much easier. In the system with competing Zn and Pb sorption, the sorption of both the ions is reduced due to competition for access to the active sites in the surface layer [47].

For Cu sorption onto hemp-based material, the sorption mechanism was different based on the modification method. For sodium carbonate-activated hemp shives, copper was adsorbed in the surface layer and diffused into the cell wall. For polycarboxylic agent-grafted hemp shives, chemisorption and ion-exchange occurred and copper was preferentially adsorbed on the surface of the inner vessel wall [48]. The size of sorbents was not discussed so it may be assumed that the cause of these differences was only the different chemical modification. In KMnO₄ modified biochar derived from walnut shell Cu was adsorbed mainly by replacing the Mn²⁺ in O-Mn and formed complexes with the surface functional groups (-OH, -COOH) according to FTIR and XPS analysis [49].

As discussed above, there is another parameter that might affect the sorption process—the adsorbed ion itself. However, the difference in the properties of the adsorbed Cu and Zn ions is insignificant (Table 6). As the ionic radius of Cu and Zn atoms are almost the same, this parameter might not influence the sorption capacity of zeolite.

Table 6. Basic characteristics of Cu and Zn ions [29,50–52].

Parameter	Cu ²⁺	Zn ²⁺
Atomic weight (g·mol ⁻¹)	63.55	65.38
Ionic radius (nm)	0.073	0.074
Hydrated ion radius (nm)	0.419	0.430
Hydration enthalpies (kJ·mol ⁻¹)	−2010	−1955
Electronegativity ¹	2.00	1.65

¹ Pauling scale.

The samples for XPS and XRF analysis were selected so that the maximum sorption capacity had been reached based on the theory of sorption. More than 95% of Cu and Zn is removed by sorption on both the zeolites.

As raw zeolites contain no Cu or Zn a comparison of Fe, Ca, Se and K content before and after the sorption is available in Table 7. A comparison of Cu or Zn to Fe, Ca, Se and K ratios are also available in Table 8. In general, Cu ions occupy the vacancies after Fe and Ca to a large extent, and K to a lesser extent. More Fe and Ca is released from the bulk, but more K is released from the surface layer. Zn ions occupy the vacancies after Fe mostly, and Se and K to a lesser extent. Fe, Se and K are equally released from the bulk and the surface layer (Table 9).

Table 7. A comparison of elemental content after: before sorption ratio.

Element	Method	Z-M20		Z-M50		Z-M20		Z-M50	
		CuSO ₄	Cu(NO ₃) ₂	CuSO ₄	Cu(NO ₃) ₂	ZnSO ₄	Zn(NO ₃) ₂	ZnSO ₄	Zn(NO ₃) ₂
Fe	XPS	0.12	0.25	0.09	0.72	0.03	0.07	0.05	0.04
	XRF	0.37	0.75	0.28	0.95	0.04	0.07	0.06	0.08
Ca	XPS	0.65	0.66	0.37	0.40	0.98	1.01	0.99	1.01
	XRF	0.77	0.77	0.66	0.77	1.00	1.03	1.10	1.07
Se	XPS	0.95	0.96	0.99	0.98	0.92	1.01	0.96	1.03
	XRF	0.99	0.98	0.92	0.92	0.96	0.95	0.89	0.88
K	XPS	0.91	0.91	0.18	0.17	0.98	0.98	0.87	1.00
	XRF	0.83	0.82	0.96	1.04	0.96	0.88	0.92	1.01

Table 8. A comparison of elemental content ratio of Cu or Zn to other elements after sorption.

Element	Method	Z-M20		Z-M50		Z-M20		Z-M50	
		CuSO ₄	Cu(NO ₃) ₂	CuSO ₄	Cu(NO ₃) ₂	ZnSO ₄	Zn(NO ₃) ₂	ZnSO ₄	Zn(NO ₃) ₂
Fe	XPS	1.26	1.21	9.82	10.00	4.17	4.18	2.02	2.00
	XRF	0.38	0.39	0.83	0.86	4.23	4.27	3.82	3.74
Ca	XPS	0.11	0.23	0.51	3.82	0.08	0.15	0.11	0.22
	XRF	0.10	0.21	0.07	0.22	0.09	0.16	0.04	0.15
Se	XPS	0.49	1.00	0.92	7.44	0.50	0.92	0.56	1.06
	XRF	0.51	1.07	0.06	0.21	0.57	1.08	0.05	0.21
K	XPS	0.09	0.19	0.77	6.47	0.08	0.17	0.10	0.17
	XRF	0.11	0.22	0.04	0.12	0.10	0.21	0.03	0.12

Table 9. The concentration of elements in posttreatment solution.

Element	Z-M20		Z-M50		Z-M20		Z-M50	
	CuSO ₄	Cu(NO ₃) ₂	CuSO ₄	Cu(NO ₃) ₂	ZnSO ₄	Zn(NO ₃) ₂	ZnSO ₄	Zn(NO ₃) ₂
Fe (mg·L ⁻¹)	62.12	52.80	16.80	5.10	67.80	65.30	13.60	8.50
Ca (mg·L ⁻¹)	46.98	45.60	55.90	53.60	2.60	2.00	0.80	1.30
Se (mg·L ⁻¹)	1.00	0.80	0.20	0.40	1.70	0.30	0.70	0.50
K (mg·L ⁻¹)	10.90	11.30	96.80	97.80	2.40	2.60	15.10	0.30

The Cu and Zn sorption capacities of studied zeolites are lower than the ones of compared sorbents (Tables 10 and 11, respectively).

Table 10. A comparison of sorption capacities of different Cu sorbents.

Sorbent	Cu Source	q_{mr} (mg·g ⁻¹)	Temperature (°C)	Initial pH	Source
Zeolite—M20	CuSO ₄	1.0619	25	*	**
Zeolite—M20	Cu(NO ₃) ₂	2.3518	25	*	**
Zeolite—M50	CuSO ₄	0.4512	25	*	**
Zeolite—M50	Cu(NO ₃) ₂	1.6745	25	*	**
magnetic nano-zeolite	Cu(NO ₃) ₂	59.90	25	9	[22]
zeolite from Kamchatka	CuSO ₄	1.46	20	low	[26]
Faujasite type zeolite	Cu(NO ₃) ₂	94.46	25	5.6	[53]
NaP zeolite from waste lithium-silicon-powder	Cu(NO ₃) ₂	62.30	25	6.0	[23]
Fly ash and NaOH synthesized zeolite	Cu(NO ₃) ₂	310.00	25	5.5	[46]
NaX nano-zeolite	N/A	111.84	25	6.5	[24]
FAU-type zeolites from coal fly ash	Cu(NO ₃) ₂	57.80	room	N/A	[27]

* No pH adjustment. ** this study.

Table 11. A comparison of sorption capacities of different Zn sorbents.

Sorbent	Zn Source	q_m , (mg·g ⁻¹)	Temperature (°C)	Initial pH	Source
Zeolite—M20	ZnSO ₄	1.1541	25	*	**
Zeolite—M20	Zn(NO ₃) ₂	2.2862	25	*	**
Zeolite—M50	ZnSO ₄	0.3928	25	*	**
Zeolite—M50	Zn(NO ₃) ₂	1.5074	25	*	**
Na-X zeolite	Zn(NO ₃) ₂	332.51	N/A	5.0	[47]
natural zeolite	Zn(NO ₃) ₂	7.57	20	*	[29]
Zeolite 3A	Zn(NO ₃) ₂	31.11	20	*	[29]
Zeolite 10A	Zn(NO ₃) ₂	34.30	20	*	[29]
Zeolite 13X	Zn(NO ₃) ₂	11.07	20	*	[29]
FAU-type zeolites from coal fly ash	Zn(NO ₃) ₂	36.77	room	N/A	[27]

* No pH adjustment. ** this study.

This study contributes to knowledge on sorption, despite low capacities, by study of not only the aqueous phase but also the solid phase. The removal of dimethyl disulfide was studied by adsorption on the ion-exchanged Y zeolites. The solid phase was studied by XRF, XRD, TGA and XPS. The optimal saturated capacity was 157.4 mg S g⁻¹ adsorbent [54]. The removal of Hg was studied by adsorption onto Co and Mn oxide-modified layered ITQ-2 zeolites. The adsorption capacity of the 5%Mn/ITQ-2 zeolite at 300 °C was 2.04 mg·g⁻¹ in 600 min [55]. Additionally, the removal of Cu by adsorption onto synthesized zeolites through fusion of lignite fly ash and NaOH or KOH pellets at 600 °C was studied using XRF, XRD, FTIR, SEM/EDS and XPS. The analyses confirmed the presence of Cu on the zeolite surface and the possible formation of CuO and/or Cu-Cl but the particle size is below 118–223 μm [44]. Synthesized natural clinoptilolite-rich zeolite with a bio-inspired adhesive, polydopamine showed slightly higher sorption capacity of 28.58 mg·g⁻¹ than the natural form of 14.93 mg·g⁻¹. The solid phase was also analyzed using FTIR, XPS and TGA [56]. Another low capacity (6.25 mg·g⁻¹) mineral studied in the process of adsorptive desulfurization of petroleum refining fractions was palygorskite, a low-cost clay mineral. It was also studied by XRF, XPS, XRD, FTIR and SEM reporting that an interaction between adsorbate/adsorbent involves π-complexation mainly with Fe species [57]. NaP1 zeolite prepared by alkali fusion and hydrothermal method from red mud was used for adsorption of methylene blue with a maximum sorption capacity of 48.7 mg·g⁻¹. Based on FTIR and XPS analyses, the possible adsorption mechanism was revealed [58]. As documented by the above studies, the sorption capacities of natural, modified and synthetic sorbents based not only on zeolites (clinoptilolite) are different based also on the removed component, though the modified versions do not often have much higher capacities. This study also contributes to unveiling the sorption process onto zeolite as different conditions of the sorption process, such as particle size distribution, pH, temperature, ion radius, etc., may significantly influence the whole sorption process and therefore also the sorption capacity. This study concentrated on the sorption process at the conditions that were not changed. This fact may minimize the need of other substances, especially those with negative environmental impact (acids and bases) as well as minimize other physical and chemical processes for pre-treatment of sorbent or sorbate, though this is not the subject of the study.

At solution pH lower than 7, the case of Cu and Zn sorption onto zeolites, hydrogen cation and heavy metal ions might compete in the sorption process, thus decreasing the heavy metal sorption capacity. In contrast, at high solution pH, hydroxide anions react with heavy metal ions and precipitate, causing fake high sorption efficiency [22].

Though the desorption process of Cu and Zn from zeolites was studied, it might be a part of further study and might bring further views into the sorption process. The experiments with simultaneous sorption of Cu and Zn might also be added to study the competitive sorption of the two metals.

5. Conclusions

The study of Cu(II) and Zn(II) removal from wastewater is crucial as discharged untreated water with excessive amount may cause high risk to the aquatic environment. The use of zeolite from Slovakia, natural material from local sources, for the sorption is an advantage. Available methods and techniques for study of both the aqueous and solid phases were used for the removal of Cu and Zn by zeolite. According to the analyses, the surface participation, electrostatic interaction, and ion exchange might also play an important role. The studied zeolites are suitable for Cu and Zn sorption as the maximum sorption capacities are in the range of 0.3928–2.3518 mg·g⁻¹. The maximum sorption capacities are higher for sulfates and the sorbent with smaller particle size (Z-M20) yet the difference between Cu and Zn sorption is insignificant for corresponding anion and particle size distribution. The content of both Cu and Zn in the surface layer and the bulk are the same for sorption onto sorbent with smaller particle size, but are higher in the surface layer than in the bulk for sorption onto sorbent with larger particle size. All the findings might imply that not only the adsorbed heavy metal affects the sorption process, but also the sorbent by its particle size, pore distribution, etc. In summary, the studied zeolites (Micro-20 and Micro-50) are environmentally friendly materials that might be used as sorbents for Cu and Zn ions from polluted wastewater. Usually, the natural forms of sorbents have lower capacities than their modified versions. The future study might concentrate on the ways of zeolite modification to increase the sorption capacity and thus the applicability of zeolite. Additionally, the economic insight into the use of zeolites for Cu and Zn adsorption and a comparison with other zeolites (natural from other localities or synthetic) might be studied to prove whether the low sorption capacity is a disadvantage of the studied zeolite usage.

Author Contributions: Conceptualization, T.B., H.P. and K.K.; methodology, T.B.; validation, T.B., H.P. and K.K.; formal analysis, T.B. and H.P.; investigation, T.B.; resources, T.B., H.P. and K.K.; data curation, T.B. and K.K.; writing—original draft preparation, T.B., H.P., K.K. and Z.H.; writing—review and editing, T.B., H.P., K.K. and Z.H.; visualization, T.B., H.P., K.K. and Z.H. All authors have read and agreed to the published version of the manuscript.

Funding: This research was funded by Kultúrna a edukačná grantová agentúra MŠVVaŠ SR, grant number 001UVLF-4/2020.

Institutional Review Board Statement: Not applicable.

Informed Consent Statement: Not applicable.

Data Availability Statement: Not applicable.

Acknowledgments: Authors would like to acknowledge support with measuring XPS and XRF data.

Conflicts of Interest: The authors declare no conflict of interest.

References

1. Zeocem®. Available online: <https://www.zeocem.com/en/> (accessed on 20 February 2022).
2. Kolarova, N.; Napiórkowski, P. Trace elements in aquatic environment. Origin, distribution, assessment and toxicity effect for the aquatic biota. *Ecohydrol. Hydrobiol.* **2021**, *21*, 655–668. [[CrossRef](#)]
3. Jan, A.T.; Azam, M.; Siddiqui, K.; Ali, A.; Choi, I.; Haq, Q.M.R. Heavy Metals and Human Health: Mechanistic Insight into Toxicity and Counter Defense System of Antioxidants. *Int. J. Mol. Sci.* **2015**, *16*, 29592–29630. [[CrossRef](#)] [[PubMed](#)]
4. Qasem, N.A.A.; Mohammed, R.H.; Lawal, D.U. Removal of heavy metal ions from wastewater: A comprehensive and critical review. *NPJ Clean Water* **2021**, *4*, 36. [[CrossRef](#)]
5. Janyasuthiwong, S.; Rene, E.R.; Esposito, G.; Lens, P.N.L. Effect of pH on Cu, Ni and Zn removal by biogenic sulfide precipitation in an inversed fluidized bed bioreactor. *Hydrometallurgy* **2015**, *158*, 94–100. [[CrossRef](#)]
6. Lewis, A.E. Review of metal sulphide precipitation. *Hydrometallurgy* **2010**, *104*, 222–234. [[CrossRef](#)]
7. Bakalár, T.; Búgel, M.; Müller, G. Influence of Zinc Adsorption on Permeate Flux through Ceramic Membrane. In Proceedings of the 2013 International Conference on Material Science and Environmental Engineering (MSEE 2013), Wuhan, China, 17–18 August 2013.

8. Lebron, Y.A.R.; Moreira, V.R.; Amaral, M.C.S. Metallic ions recovery from membrane separation processes concentrate: A special look onto ion exchange resins. *Chem. Eng. J.* **2021**, *425*, 131812. [[CrossRef](#)]
9. Marder, L.; Benvenuti, T.; Giacobbo, A.; Rodrigues, M.A.S.; Ferreira, J.Z.; Bernardes, A.M. Membranes for Heavy Metals Removal. In *Remediation of Heavy Metals. Environmental Chemistry for a Sustainable World*, 1st ed.; Inamuddin, Ahamed, M.I., Lichtfouse, E., Altalhi, T., Eds.; Springer: Cham, Germany, 2021; Volume 70, pp. 135–156.
10. Nyström, F.; Nordqvist, K.; Herrmann, I.; Hedström, A.; Viklander, M. Removal of metals and hydrocarbons from stormwater using coagulation and flocculation. *Water Res.* **2020**, *182*, 115919. [[CrossRef](#)]
11. Hargreaves, A.J.; Vale, P.; Whelan, J.; Alibardi, L.; Constantino, C.; Dotro, G.; Cartmell, E.; Campo, P. Coagulation–flocculation process with metal salts, synthetic polymers and biopolymers for the removal of trace metals (Cu, Pb, Ni, Zn) from municipal wastewater. *Clean Technol. Environ. Policy* **2018**, *20*, 393–402. [[CrossRef](#)]
12. Sabo, Š.; Bakalár, T.; Búgel, M.; Pavolová, H. Biosorption of copper by eggshell from aqueous solutions. In Proceedings of the SGEM 2014: 14th International Multidisciplinary Scientific Geoconference: GeoConference on Ecology, Economics, Education and Legislation, Albena, Bulgaria, 17–26 June 2014.
13. Bashir, A.; Malik, L.A.; Ahad, S.; Manzoor, T.; Bhat, M.A.; Dar, G.N.; Pandith, A.H. Removal of heavy metal ions from aqueous system by ion-exchange and biosorption methods. *Environ. Chem. Lett.* **2019**, *17*, 729–754. [[CrossRef](#)]
14. Peng, S.; Wang, R.; Yang, L.; He, L.; He, X.; Liu, X. Biosorption of copper, zinc, cadmium and chromium ions from aqueous solution by natural foxtail millet shell. *Ecotoxicol. Environ. Saf.* **2018**, *165*, 61–69. [[CrossRef](#)]
15. De Luca, P.; Bernaudo, I.; Elliani, R.; Tagarelli, A.; Nagy, J.B.; Macario, A. Industrial Waste Treatment by ETS-10 Ion Exchanger Material. *Materials* **2018**, *11*, 2316. [[CrossRef](#)] [[PubMed](#)]
16. Bakalár, T.; Pavolová, H.; Búgel, M. Influence of NaNO₃ and NaCl on Copper Removal from Aqueous Solutions by Natural Zeolite. *Adv. Sci. Lett.* **2013**, *19*, 325–328. [[CrossRef](#)]
17. Bakalár, T.; Pavolová, H. Application of organic waste for adsorption of Zn(II) and Cd(II) ions. *Environ. Prot. Eng.* **2019**, *45*, 35–54. [[CrossRef](#)]
18. Bakalár, T.; Pavolová, H.; Kaňuchová, M. Removal of Cu and Zn Ions from Solutions Using Sludge from Drinking Water Treatment. *Chem. Listy* **2017**, *111*, 269–274.
19. Mavrov, V.; Erwe, T.; Blöcher, C.; Chmiel, H. Study of new integrated processes combining adsorption, membrane separation and flotation for heavy metal removal from wastewater. *Desalination* **2003**, *157*, 97–104. [[CrossRef](#)]
20. Younas, F.; Mustafa, A.; Farooqi, Z.U.R.; Wang, X.; Younas, S.; Mohy-Ud-Din, W.; Ashir Hameed, M.; Mohsin Abrar, M.; Maitlo, A.A.; Noreen, S.; et al. Current and Emerging Adsorbent Technologies for Wastewater Treatment: Trends, Limitations, and Environmental Implications. *Water* **2021**, *13*, 215. [[CrossRef](#)]
21. Chai, W.S.; Cheun, J.Y.; Kumar, P.S.; Mubashir, M.; Majeed, Z.; Banat, F.; Ho, H.; Show, P.L. A review on conventional and novel materials towards heavy metal adsorption in wastewater treatment application. *J. Clean. Prod.* **2021**, *296*, 126589. [[CrossRef](#)]
22. Zhang, X.; Cheng, T.; Chen, C.; Wang, L.; Deng, Q.; Chen, G.; Ye, C. Synthesis of a novel magnetic nano-zeolite and its application as an efficient heavy metal adsorbent. *Mater. Res. Express* **2020**, *7*, 085007. [[CrossRef](#)]
23. Pu, X.; Yao, L.; Yang, L.; Jiang, W.; Jiang, X. Utilization of industrial waste lithium-silicon-powder for the fabrication of novel nap zeolite for aqueous Cu(II) removal. *J. Clean. Prod.* **2020**, *265*, 121822. [[CrossRef](#)]
24. Yurekli, Y. Determination of adsorption characteristics of synthetic NaX nanoparticles. *J. Hazard. Mater.* **2019**, *378*, 120743. [[CrossRef](#)]
25. Bai, S.; Chu, M.; Zhou, L.; Chang, Z.; Zhang, C.; Liu, B. Removal of heavy metals from aqueous solutions by X-type zeolite prepared from combination of oil shale ash and coal fly ash. *Energy Sources Part A* **2019**. [[CrossRef](#)]
26. Belova, T.P. Adsorption of heavy metal ions (Cu²⁺, Ni²⁺, Co²⁺ and Fe²⁺) from aqueous solutions by natural zeolite. *Heliyon* **2019**, *5*, e02320. [[CrossRef](#)] [[PubMed](#)]
27. Joseph, I.V.; Tosheva, L.; Doyle, A.M. Simultaneous removal of Cd(II), Co(II), Cu(II), Pb(II), and Zn(II) ions from aqueous solutions via adsorption on FAU-type zeolites prepared from coal fly ash. *J. Environ. Chem. Eng.* **2020**, *8*, 103895. [[CrossRef](#)]
28. Abollino, O.; Giacomino, A.; Malandrino, M.; Mentasti, E. Interaction of metal ions with montmorillonite and vermiculite. *Appl. Clay Sci.* **2008**, *38*, 227–236. [[CrossRef](#)]
29. Kozera-Sucharda, B.; Gworek, B.; Kondzielski, I. The Simultaneous Removal of Zinc and Cadmium from Multicomponent Aqueous Solutions by Their Sorption onto Selected Natural and Synthetic Zeolites. *Minerals* **2020**, *10*, 343. [[CrossRef](#)]
30. Semenkova, A.; Belousov, P.; Rzhavskaia, A.; Izosimova, Y.; Maslakov, K.; Tolpeshta, I.; Romanchuk, A.; Krupskaya, V. U(VI) sorption onto natural sorbents. *J. Radioanal. Nucl. Chem.* **2020**, *326*, 293–301. [[CrossRef](#)]
31. Inglezakis, V.J.; Satayeva, A.; Yagofarova, A.; Tauanov, Z.; Meiramkulova, K.; Farrando-Pérez, J.; Bear, J.C. Surface Interactions and Mechanisms Study on the Removal of Iodide from Water by Use of Natural Zeolite-Based Silver Nanocomposites. *Nanomaterials* **2020**, *10*, 1156. [[CrossRef](#)]
32. Bandura, L.; Panek, R.; Madej, J.; Franus, W. Synthesis of zeolite-carbon composites using high-carbon fly ash and their adsorption abilities towards petroleum substances. *Fuel* **2021**, *283*, 119173. [[CrossRef](#)]
33. Vergara-Figueroa, J.; Alejandro-Martín, S.; Pesenti, H.; Cerda, F.; Fernández-Pérez, A.; Gacitúa, W. Obtaining Nanoparticles of Chilean Natural Zeolite and its Ion Exchange with Copper Salt (Cu²⁺) for Antibacterial Applications. *Materials* **2019**, *12*, 2202. [[CrossRef](#)]

34. Hong, M.; Yu, L.; Wang, Y.; Zhang, J.; Chen, Z.; Dong, L.; Zan, Q.; Li, R. Heavy metal adsorption with zeolites: The role of hierarchical pore architecture. *Chem. Eng. J.* **2019**, *359*, 363–372. [[CrossRef](#)]
35. Öztaş, N.A.; Karabakan, A.; Topal, Ö. Removal of Fe(III) ion from aqueous solution by adsorption on raw and treated clinoptilolite samples. *Microporous Mesoporous Mater.* **2008**, *111*, 200. [[CrossRef](#)]
36. Freundlich, H.M.F. Über die Adsorption in Lösungen. *Z. Phys. Chem.* **2017**, *57*, 385–470. [[CrossRef](#)]
37. Albadarin, A.B.; Al-Muhtaseb, A.H.; Al-laqtah, N.A.; Walke, G.M.; Allen, S.J.; Ahmad, M.N.M. Biosorption of toxic chromium from aqueous phase by lignin: Mechanism, effect of other metal ions and salts. *Chem. Eng. J.* **2011**, *169*, 20. [[CrossRef](#)]
38. Langmuir, I. The constitution and fundamental properties of solids and liquids. Part, I. Solids. *J. Am. Chem. Soc.* **1916**, *38*, 2221. [[CrossRef](#)]
39. Günay, A.; Arslankaya, E.; Tosun, I. Lead removal from aqueous solution by natural and pretreated clinoptilolite: Adsorption equilibrium and kinetics. *J. Hazard. Mater.* **2007**, *146*, 362. [[CrossRef](#)]
40. Redlich, O.; Peterson, D.L. A useful adsorption isotherm. *J. Phys. Chem.* **1959**, *63*, 1024. [[CrossRef](#)]
41. Hüfner, S. *Photoelectron Spectroscopy: Principles and Applications*, 3rd ed.; Springer: Berlin, Germany, 2003; pp. 173–210, 411–500.
42. Caridi, F.; Torrisi, L.; Cutroneo, M.; Barreca, F.; Gentile, C.; Serafino, T.; Castrizio, D. XPS and XRF depth patina profiles of ancient silver coins. *Appl. Surf. Sci.* **2013**, *272*, 82–87. [[CrossRef](#)]
43. Bakalár, T.; Kaňuchová, M.; Girová, A.; Pavolová, H.; Hromada, R.; Hajduová, Z. Characterization of Fe(III) Adsorption onto Zeolite and Bentonite. *Int. J. Environ. Res. Public Health* **2020**, *17*, 5718. [[CrossRef](#)]
44. Malara, C.; Pierini, G.; Viola, A. *Correlation, Analysis and Prediction of Adsorption Equilibria*; Report EUR 13996 EN; European Commission: Luxembourg, 1992.
45. Ayawei, N.; Ebelegi, A.N.; Wankasi, D. Modelling and Interpretation of Adsorption Isotherms. *J. Chem.* **2017**, *2017*, 3039817. [[CrossRef](#)]
46. Vavouraki, A.; Bartzas, G.; Komnitsas, K. Synthesis of Zeolites from Greek Fly Ash and Assessment of Their Copper Removal Capacity. *Minerals* **2020**, *10*, 844. [[CrossRef](#)]
47. Panek, R.; Medykowska, M.; Wiśniewska, M.; Szewczuk-Karpisz, K.; Jędruchiewicz, K.; Franus, M. Simultaneous Removal of Pb²⁺ and Zn²⁺ Heavy Metals Using Fly Ash Na-X Zeolite and Its Carbon Na-X(C) Composite. *Materials* **2021**, *14*, 2832. [[CrossRef](#)] [[PubMed](#)]
48. Mongioví, C.; Crini, G.; Gabrion, X.; Placet, V.; Blondeau-Patissier, V.; Krystianiak, A.; Durand, S.; Beaugrand, J.; Dorlando, A.; Rivard, C.; et al. Revealing the adsorption mechanism of copper on hemp-based materials through EDX, nano-CT, XPS, FTIR, Raman, and XANES characterization techniques. *Chem. Eng. J. Adv.* **2022**, *10*, 100282. [[CrossRef](#)]
49. Chen, S.; Zhong, M.; Wang, H.; Zhou, S.; Li, W.; Wang, T.; Li, J. Study on adsorption of Cu²⁺, Pb²⁺, Cd²⁺, and Zn²⁺ by the KMnO₄ modified biochar derived from walnut shell. *Int. J. Environ. Sci. Technol.* **2022**. [[CrossRef](#)]
50. Zhu, C.; Dong, X.; Chen, Z.; Naidu, R. Adsorption of aqueous Pb(II), Cu(II), Zn(II) ions by amorphous tin(VI) hydrogen phosphate: An excellent inorganic adsorbent. *Int. J. Environ. Sci. Technol.* **2016**, *13*, 1257–1268. [[CrossRef](#)]
51. Yoder, C.H. *Ionic Compounds: Applications of Chemistry to Mineralogy*, 1st ed.; John Wiley & Sons, Inc.: Hoboken, NJ, USA, 2006.
52. Goel, J.; Kadirvelu, K.; Rajagopal, C. Competitive Sorption of Cu(II), Pb(II) and Hg(II) Ions from Aqueous Solution Using Coconut Shell-based Activated Carbon. *Adsorpt. Sci. Technol.* **2004**, *22*, 257–273. [[CrossRef](#)]
53. Chen, Y.; Armutlulu, A.; Sun, W.; Jiang, W.; Jiang, X.; Lai, B.; Xie, R. Ultrafast removal of Cu(II) by a novel hierarchically structured faujasite-type zeolite fabricated from lithium silica fume. *Sci. Total Environ.* **2020**, *714*, 136724. [[CrossRef](#)]
54. Yi, D.; Huang, H.; Meng, X.; Shi, L. Adsorption-desorption behavior and mechanism of dimethyl disulfide in liquid hydrocarbon streams on modified Y zeolites. *Appl. Catal. B* **2014**, *148–149*, 377–386. [[CrossRef](#)]
55. Ma, Y.; Xu, T.; Zhang, X.; Wang, J.; Xu, H.; Huang, W.; Zhang, H. Excellent adsorption performance and capacity of modified layered ITQ-2 zeolites for elemental mercury removal and recycling from flue gas. *J. Hazard. Mater.* **2022**, *423*, 127118. [[CrossRef](#)]
56. Yu, Y.; Shapter, J.G.; Popelka-Filcoff, R.; Bennett, J.W.; Ellis, A.V. Copper removal using bio-inspired polydopamine coated natural zeolites. *J. Hazard. Mater.* **2014**, *273*, 174–182. [[CrossRef](#)]
57. Câmara, A.B.F.; Sales, R.V.; Bertolino, L.C.; Furlanetto, R.P.P.; Rodríguez-Castellón, E.; de Carvalho, L.S. Novel application for palygorskite clay mineral: A kinetic and thermodynamic assessment of diesel fuel desulfurization. *Adsorption* **2020**, *26*, 267–282. [[CrossRef](#)]
58. Cheng, Y.; Xu, L.; Liu, C. NaP1 zeolite synthesized via effective extraction of Si and Al from red mud for methylene blue adsorption. *Adv. Powder Technol.* **2021**, *32*, 3904–3914. [[CrossRef](#)]